Eur Radiol (2015) 25:2859–2868
DOI 10.1007/s00330-015-3686-3

HEPATOBILIARY-PANCREAS

Noninvasive diagnosis of hepatocellular carcinoma on gadoxetic acid-enhanced MRI: can hypointensity on the hepatobiliary phase be used as an alternative to washout?

Ijin Joo · Jeong Min Lee · Dong Ho Lee · Ju Hyeon Jeon · Joon Koo Han · Byung Ihn Choi

Received: 29 August 2014 / Revised: 3 January 2015 / Accepted: 19 February 2015 / Published online: 14 March 2015

Abstract
Objectives To determine which dynamic phase(s) of gadoxetic acid-enhanced MRI is most appropriate to assess "washout" in the noninvasive diagnosis of hepatocellular carcinoma (HCC) based on hemodynamic pattern.
Methods In this retrospective cohort study, 288 consecutive patients with chronic liver disease presented with 387 arterially enhancing nodules (292 HCCs, 95 non-HCCs) (≥1 cm) on gadoxetic acid-enhanced MRI. All HCCs were confirmed by histopathology or by their typical enhancement pattern on dynamic liver CT. MR imaging diagnosis of HCC was made using criteria of arterial enhancement and hypointensity relative to the surrounding parenchyma (1) on the portal-venous phase (PVP), (2) on the PVP and/or transitional phase (TP), or (3) on the PVP and/or TP, and/or hepatobiliary phase (HBP).
Results For the noninvasive diagnosis of HCC, criterion 1 provided significantly higher specificity (97.9 %; 95 % confidence interval, 92.6 – 99.7 %) than criteria 2 (86.3 %; 77.7 – 92.5 %), or 3 (48.4 %; 38.0 – 58.9 %). Conversely, higher sensitivity was obtained with criterion 3 (93.8 %; 90.4 – 96.3 %) than with criterion 2 (86.6 %; 82.2 – 90.3 %) or 1 (70.9 %; 65.3 – 76.0 %).
Conclusions To make a sufficiently specific diagnosis of HCC using gadoxetic acid-enhanced MRI based on typical enhancement features, washout should be determined on the PVP alone rather than combined with hypointensity on the TP or HBP.
Key points
- *Gadoxetic acid-enhanced MRI enhancement features can be used to diagnose HCC.*
- *Washout should be determined on the PVP alone for high specificity.*
- *Hypointensity on the TP or HBP increases sensitivity but lowers specificity.*

Keywords Hepatocellular carcinoma (HCC) · Gadoxetic acid (Gd-EOB-DTPA) · MRI · Liver · Diagnostic efficacy

Abbreviations

HCC	hepatocellular carcinoma
HAP	hepatic arterial phase
PVP	portal-venous phase
TP	transitional phase
HBP	hepatobiliary phase

Introduction

According to the current guidelines on the management of hepatocellular carcinoma (HCC), for hepatic nodules larger than 1 cm in patients with cirrhosis or chronic liver disease (CLD), HCC can be diagnosed without requirement of biopsy if the typical dynamic enhancement pattern, i.e., hypervascularity on the hepatic arterial phase (HAP) and washout on a later phase, is present in dynamic contrast-enhanced CT and/or MRI [1–5]. Recently, the accumulating evidence appears to suggest that MRI using hepatobiliary

I. Joo · J. M. Lee · D. H. Lee · J. H. Jeon · J. K. Han · B. I. Choi
Department of Radiology, Seoul National University Hospital, 101 Daehak-ro, Jongno-gu Seoul 110-744, Korea

I. Joo · J. M. Lee · D. H. Lee · J. H. Jeon · J. K. Han · B. I. Choi
Department of Radiology, Seoul National University College of Medicine, 103 Daehak-ro, Jongno-gu Seoul 110-799, Korea

J. M. Lee (✉) · J. K. Han · B. I. Choi
Institute of Radiation Medicine, Seoul National University Medical Research Center, 103 Daehak-ro, Jongno-gu Seoul 110-799, Korea
e-mail: jmsh@snu.ac.kr

agents such as gadoxetic acid may be a more sensitive method for the detection of small HCCs than extracellular contrast media (ECCM)-enhanced CT or MRI [6–9]. This higher sensitivity is mainly attributable to the dual properties of gadoxetic acid which provides vascular phase information as well as additional information regarding the hepatobiliary phase (HBP) by its uptake into hepatocytes [10]. However, at present, the major guidelines proposed by the American Association for the Study of Liver Diseases (AASLD) in 2010 and the European Association for the Study of the Liver (EASL) in 2012 include ECCM-enhanced CT and MRI, not gadoxetic acid-enhanced MRI, as the standard methods for evaluating the vascular pattern of hepatic nodules [3, 11].

Despite the fact that the HBP of gadoxetic acid-enhanced MRI has been reported to facilitate the detection of small HCCs [9, 12–14] and to help differentiate HCCs from hypervascular pseudolesions [15, 16], hypointensity on the HBP or transitional phase (TP, 3-min delay) is a major problem in the interpretation of cirrhotic nodules based on their enhancement pattern [17]. This is because hypointensity on the TP and HBP of gadoxetic acid-enhanced MRI has a different meaning from the hypointensity observed on ECCM-enhanced imaging [18, 19]. For example, as the uptake of gadoxetic acid by hepatocytes starts approximately 90 s after contrast injection, the tumor-to-liver contrast in the TP would be derived not only from true washout of the contrast agents, but also from prominent enhancement of the surrounding hepatic parenchyma [18, 19]. Therefore, determining whether or not the hypointensity observed on dynamic phases and/or HBP can be used as an alternative to "washout", or in other words, which phase(s) should be included to assess "washout, " is warranted for the application of gadoxetic acid-enhanced MRI for the noninvasive diagnosis of HCC.

Therefore, the purposes of our study are to evaluate the diagnostic performance of gadoxetic acid-enhanced MRI in the noninvasive diagnosis of HCC based on current guidelines of "hypervascularity on the HAP and washout on a later phase" and to determine the most appropriate dynamic phase(s) of gadoxetic acid-enhanced MRI to assess "washout" in a retrospective cohort of patients with CLD and arterially enhancing hepatic nodules.

Materials and methods

Patients

This retrospective cohort study was approved by our institutional review board and the requirement for informed consent was waived. From September 2012 to May 2013, a total of 2,874 gadoxetic-acid enhanced MRI images were available on our picture archiving and communication system (PACS). Among them, we included patients proven to have CLD by positive serum hepatitis B and/or C viral markers, histopathology, or clinical diagnosis of liver cirrhosis [20], in whom arterially enhancing hepatic nodules measuring 1 cm or larger in diameter were detected during imaging surveillance and in whom the final diagnosis was confirmed as either HCCs or non-HCCs. Accordingly, we excluded 2,404 cases upon review of their MRI reports and the electronic medical records (EMR) of each case. Reasons for exclusion with the corresponding numbers of patients are listed in Fig. 1. The remaining 470 scans were reviewed in consensus by two experienced radiologists (J.M.L. and I.J. with 22 and 7 years of experience in abdominal MRI). After image review of the 470 MRI scans, 182 cases which did not satisfy the inclusion criteria were additionally excluded (Fig. 1). The presence of arterial hyperenhancement was determined by visual comparison of the HAP and the unenhanced phase with additional review of subtraction images [21]. Nodules exhibiting homogeneous or variegated enhancement patterns were included while those exhibiting the ring enhancement pattern or peripheral globular enhancement pattern on the HAP were excluded [22]. Of the 288 patients enrolled in the final cohort, 227 were men and 61 were women with a mean age of 59 years (range, 21 – 85 years). Their chronic liver disease was associated with HBV (n=188), HCV (n=26), alcohol (n=34), mixed causes (e.g., HBV and alcohol) (n=6), and other reasons such as autoimmune hepatitis or unknown causes (n=34). According to the Child-Pugh classification [23], 271 patients were classified as having Child-Pugh A, eight as Child-Pugh B, and three as Child-Pugh C, and the other six were unclassified due to the lack of laboratory findings. In cases with multiple lesions satisfying the inclusion criteria, the two aforementioned radiologists (J.M.L. and I.J.) selected and annotated the target lesions in the HAP images of gadoxetic acid-enhanced MRI for a maximum of three in number per patient. Finally, a total of 387 nodules in 288 MRI scans of 288 patients were included for imaging analysis.

Lesion confirmation

Of the 387 nodules, 292 nodules were diagnosed as HCCs (mean size, 35 mm; range, 10 – 210 mm), and the other 95 nodules were determined to be non-HCCs (mean size, 20 mm; range, 10 – 125 mm). Diagnoses of the 292 HCCs were made through histopathology (n=128: surgical resection, n=115; and percutaneous biopsy, n=13), or by the typical enhancement pattern of HCCs according to the 2010 AASLD guidelines on dynamic liver CTs performed within 2 months prior to the MRI, i.e., arterial hyperenhancement and portal-venous or delayed phase washout (n=164) [2].

Of the 95 non-HCCs, all 15 malignant lesions were confirmed by histopathology (n=15: surgical resection, n=8; percutaneous biopsy, n=7). They included combined

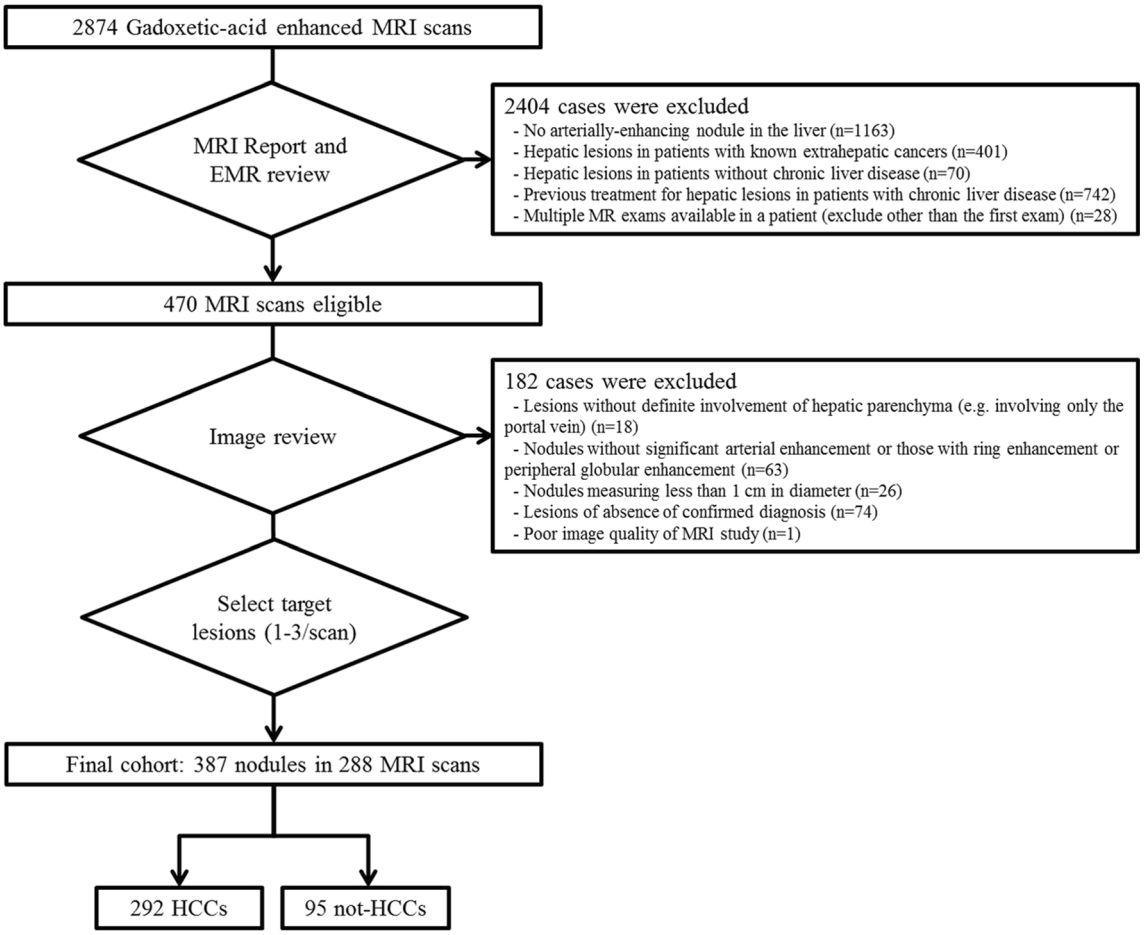

Fig. 1 Flowchart showing the study population and excluded patients

hepatocellular and cholangiocarcinomas (cHCC-CCs) (n=3), intrahepatic cholangiocarcinomas (n=10), and metastases (n=2). Of the 80 non-HCC benign nodules, benignity was confirmed in nine by histopathology (surgical resection, n=7; and percutaneous biopsy, n=2) or by characteristic imaging findings and follow-up of a minimum of 6 months (n=71). Of the nine benign lesions confirmed by histopathology, one nodule was diagnosed as an inflammatory lesion, seven were diagnosed as focal nodular hyperplasias (FNH) or FNH-like nodules based on their pathologic report, and one nodule was diagnosed as an arterioportal shunt (APS) as it was not found in the histology specimen and showed typical imaging features of APS on preoperative imaging studies described later in this paragraph. The imaging findings used for the imaging-based diagnosis of the 71 non-HCC benign lesions were as follows: for hemangioma (n=34), its classic enhancement pattern on dynamic contrast-enhanced CT or MRI and hyperintensity on T2-weighted MR imaging, without interval change during follow-up [24, 25]; for APS (n=32), isoattenuation or isointensity on dynamic CT or MRI other than HAP images, isointensity on the HBP, and no change or a decrease in size during follow-up [15, 26]; for the inflammatory lesion (n=1), conspicuity on at least one of either the portal-venous or delayed phase images different from APS, and a decrease in size or disappearance during the follow-up period [27, 28]; and for FNH or FNH-like nodules (n=4), iso- or hypersignal intensity during the portal-venous phase, at least partial hyperintensity compared to the liver parenchyma in the hepatobiliary phase, and no interval change [29]. In summary, the final diagnosis of non-HCC lesions were 15 malignant lesions including cHCC-CCs (n=3), intrahepatic cholangiocarcinomas (n=10), metastases (n=2), and 80 benign lesions including hemangiomas (n=34), APS (n=33), inflammatory lesions (n=2), and FNH or FNH-like nodules (n=11). Subgroup analyses were additionally performed for lesions diagnosed through histopathology (128 HCCs and 24 non-HCCs) in order to avoid potential false positive and false negative diagnoses from imaging-based diagnosis, and for lesions smaller than 20 mm in diameter (97 HCCs and 70 non-HCCs).

MR image acquisition

MR examinations were performed on either the 3.0 T or 1.5 T MR system available in our institution: Signa HDxt 1.5 T (GE Medical Systems, Milwaukee, WI, USA) (n=127),

Magnetom Verio or Magnetom Trio or Biograph mMR (Siemens Healthcare, Erlangen, Germany) (n=53), Ingenia 3.0 T (Philips Medical System, Best, Netherlands) (n=53), or various 3.0 T or 1.5 T scanners at an outside hospital (n=55). Routine MRI sequences included a respiratory-triggered T2-weighted fast spin echo sequence, a half-Fourier acquisition single-shot turbo spin-echo sequence (HASTE), free-breathing diffusion-weighted imaging (DWI), and a breath-hold T1-weighted spoiled dual echo (in-phase and out-of-phase) gradient recalled echo (GRE) sequence. Dynamic and HBP images were obtained using the fat-suppressed, 3D GRE sequence. Detailed parameters of the T1-weighted 3D GRE sequence are listed in Table 1. Immediately after obtaining the unenhanced T1-weighted images, 10 mL of gadoxetic acid (Primovist, Bayer Schering Pharma AG, Berlin, Germany) was administered intravenously at a rate of 1.5 mL/s, followed by a 20 mL saline flush through an antecubital venous catheter, and thereafter, multiphasic dynamic images were obtained. Scanning delay times were determined with real-time MRI fluoroscopic monitoring. Arterial phase images were obtained 7 s after contrast arrival at the distal thoracic aorta, and subsequent portal-venous phase (PVP) images were obtained approximately 50 s after beginning contrast medium injection. Thereafter, TP and HBP images were obtained 3 min and 20 min after beginning contrast medium injection, respectively. Acquisition of 3D GRE data for each dynamic phase and HBP was finished during a single breath-hold (15 – 20 s) at the end of expiration.

Image analysis

All MR images were interpreted in consensus by two abdominal radiologists (D.H.L. and J.H.J., each with 8 years of experience in the interpretation of liver MR imaging) who were blinded to whether the lesions were confirmed as HCCs or non-HCCs. For each target lesion, which was annotated on the HAP images, two radiologists evaluated whether or not the lesion showed hypointensity on the PVP, TP, and HBP images, respectively. Hypointensity on the PVP, TP, and HBP were qualitatively defined as when any part of the nodule showing arterial enhancement demonstrated a corresponding hypointense area relative to the surrounding liver parenchyma (within 3 cm from the outer border of the nodule) [30].

Statistical analysis

Based on the results of imaging interpretation, three different gadoxetic acid-enhanced MR imaging criteria for "washout on a later phase" were applied for the diagnosis of HCCs. Those MR imaging criteria were: hypervascularity on the HAP and (1) hypointensity on the PVP, (2) hypointensity on the PVP and/or TP, or (3) hypointensity on the PVP and/or TP, and/or HBP (i.e. hypointense on one or more of later phases). For each criterion, per-lesion sensitivity, specificity, and positive and negative predictive values with 95 % confidence intervals (95 % CIs), and accuracies were calculated. All statistical analyses were performed using MedCalc software version 12.4.0.0 (MedCalc Software, Mariakerke, Belgium).

Results

Frequency of hypointensity during the PVP, TP, and HBP

Of the 387 arterially enhancing nodules (292 HCCs and 95 non-HCCs) on gadoxetic acid-enhanced MRI in patients with CLD, 209 nodules (207 HCCs and two non-HCCs) (54.0 %) showed relative hypointensity compared with the surrounding parenchyma on the PVP; 264 nodules (251 HCCs and 13 non-HCCs) (68.2 %) showed hypointensity on the TP; and 318 nodules (269 HCCs and 49 non-HCCs) (82.2 %) were seen as hypointense on the HBP. Among small nodules<20 mm in diameter (n=167), 54 nodules (54 HCCs and 0 non-HCCs) (32.3 %) showed hypointensity on the PVP; 84 nodules (78 HCCs and six non-HCCs) (50.3 %) showed hypointensity on the PVP and/or TP; and 117 nodules (87 HCCs and 30 non-HCCs) (70.1 %) showed hypointensity on the PVP and/or TP, and/or HBP.

Diagnostic performance of gadoxetic acid-enhanced MRI using different criteria for "washout"

For the differential diagnosis of HCCs from other arterially enhancing nodules on gadoxetic acid-enhanced MRI, diagnostic performances of the different imaging criteria for "washout" are summarized in Table 2. Imaging criterion of "hypointensity on the PVP" provided the highest specificity (97.9 %) and highest positive predictive value (PPV) (99.0 %)

Table 1 MR Acquisition parameters of the T1-weighted 3D GRE sequence at our institution

Acquisition Parameters	3.0 T scanner	1.5 T scanner
Repetition time (ms)	3.2 - 4.3	4.5 - 5.2
Echo time (ms)	2.0 - 3.0	2.2 - 2.5
Flip angle (°)	10 - 15	12
Section thickness (mm)	5.6 - 8.0 interpolated to 2.8 - 4.0	4.8 interpolated to 1.2
Fat suppression	Yes	Yes

Table 2 Diagnostic Performances of Different Imaging Criteria for "Washout" on Gadoxetic Acid-Enhanced MRI for Hepatocellular Carcinoma

Imaging criteria	Sensitivity (%)	Specificity (%)	PPV (%)	NPV (%)	Accuracy (%)
Hyperenhancement on HAP					
+ Hypointensity on PVP	70.9 (207/292) [65.3-76.0]	97.9 (93/95) [92.6-99.7]	99.0 (207/209) [96.6-99.9]	52.2 (93/178) [44.6-59.8]	77.5 (300/387)
+ Hypointensity on PVP and/or TP	86.6 (253/292) [82.2-90.3]	86.3 (82/95) [77.7-92.5]	95.1 (253/266) [91.8-97.4]	67.8 (82/121) [58.7-76.0]	86.6 (335/387)
+ Hypointensity on PVP and/or TP, and/or HBP	93.8 (274/292) [90.4-96.3]	48.4 (46/95) [38.0-58.9]	84.8 (274/323) [80.4-88.6]	71.9 (46/64) [59.2-82.4]	82.7 (320/387)

Note: Numbers in parentheses were used to calculate percentages. Numbers in square brackets are 95 % confidence intervals. *HAP*=hepatic arterial phase, *PVP*=portal-venous phase, *TP*=transitional phase, *HBP*=hepatobiliary phase, *PPV*=positive predictive value, *NPV*=negative predictive value

for the diagnosis of HCCs, whereas criteria of "hypointensity on the PVP and/or TP" and "hypointensity on the PVP and/or TP, and/or HBP" showed lower specificities and lower PPVs of 86.3 % and 95.1 %, and 48.4 % and 84.8 %, respectively (Fig. 2).

Of the 95 non-HCCs, two lesions which showed "hypointensity on the PVP" were cHCC-CCs, while 13 lesions which showed "hypointensity on the PVP and/or TP" included cHCC-CCs (n=3) (Fig. 3), cholangiocarcinomas (n=6), metastases (n=1), and hemangiomas (n=3) (Fig. 4). Of the 292 HCCs, 274 HCCs were seen as hypointense lesions on one or more of the later phases including the PVP, TP, and HBP resulting in the highest sensitivity of 93.8 %. However, criterion of "hypointensity on the PVP and/or TP, and/or HBP" demonstrated the lowest specificity of 48.4 % as many of the non-HCCs (n=49) were seen as hypointense lesions on HBP: cHCC-CCs (n=3), cholangiocarcinomas (n=10), metastases (n=2), hemangiomas (n=32), and inflammatory lesions (n=2).

In the subgroup analysis of histopathologically confirmed lesions (128 HCCs and 24 non-HCCs), diagnostic performances of the different imaging criteria for "washout" are summarized in Table 3. In small nodules<20 mm in diameter (97 HCCs and 70 non-HCCs), imaging criterion of "hypointensity on the PVP" resulted in a sensitivity of 55.7 % (54/97) and a specificity of 100 % (70/70), whereas imaging criteria of "hypointensity on the PVP and/or TP" and "hypointensity on the PVP and/or TP, and/or HBP" resulted in sensitivities of 80.4 % (78/97) and 89.7 % (87/97), and specificities of 91.4 % (64/70) and 57.1 % (40/70), respectively. Subgroup analyses

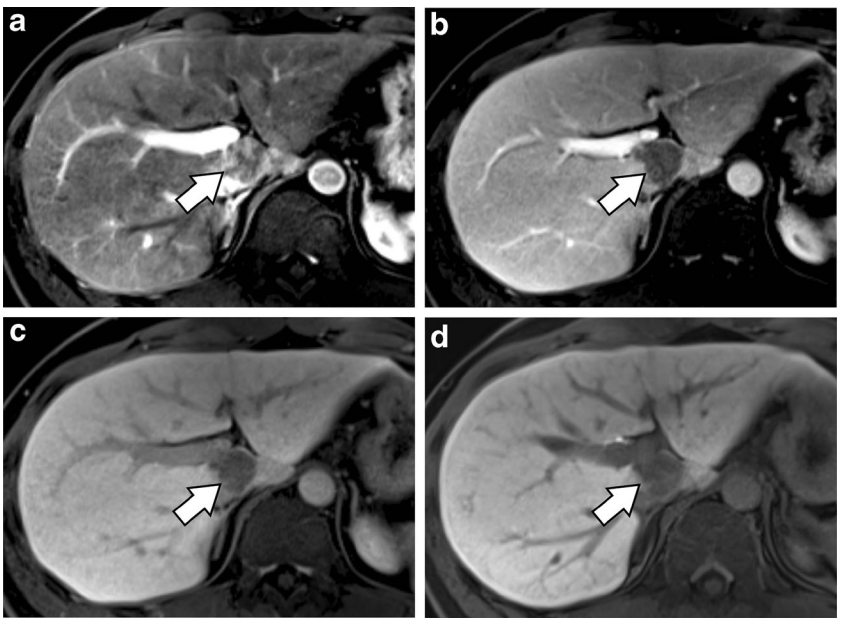

Fig. 2 A histopathologically confirmed hepatocellular carcinoma (HCC) in a 31-year-old male patient with chronic hepatitis B. On gadoxetic acid-enhanced MRI, there is an arterially enhancing nodule in the caudate lobe of the liver (**a**) showing hypointensity relative to the liver parenchyma in the portal-venous phase (PVP) (**b**) and transitional phase (TP) images (**c**) (*arrows*). (**d**) On the hepatobiliary phase (HBP) image, the nodular lesion shows hypointensity relative to the surrounding parenchyma. All imaging criteria for washout including "hypointensity on the PVP", "hypointensity on the PVP and/or TP", and "hypointensity on the PVP and/or TP, and/or HBP" can correctly diagnose this nodule as an HCC

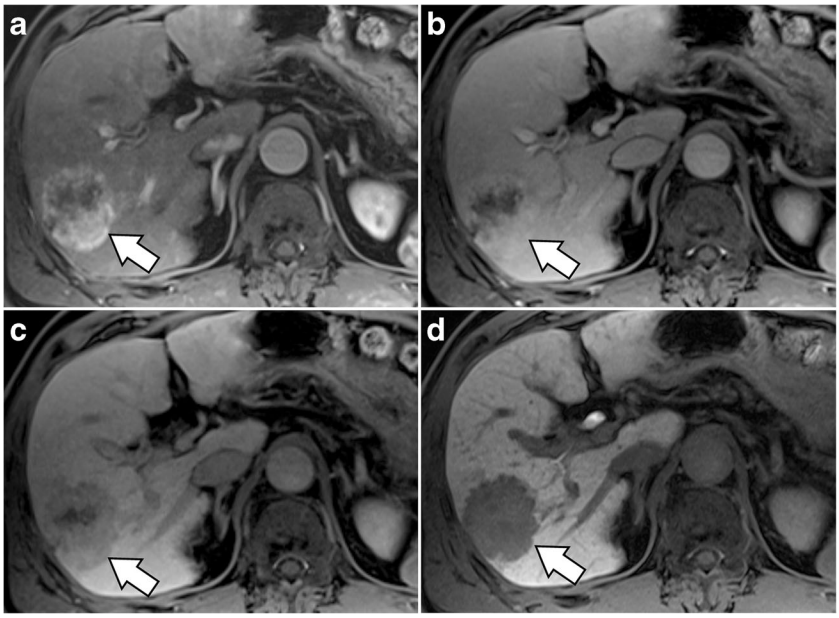

Fig. 3 A histopathologically confirmed combined hepatocellular and cholangiocarcinoma in a 60-year-old female patient with chronic hepatitis B. (**a**) On hepatic arterial phase image, a 4 cm tumour with variegated enhancement (*arrow*) is seen in segment 6 of the liver. On PVP (**b**), TP (**c**), and HBP (**d**), the arterially enhancing portion of this tumour shows iso-, hypo-, and hypointensity relative to the liver parenchyma, respectively. Criterion of "hypointensity on the PVP" would correctly diagnose this lesion as non-HCC; however, criteria of "hypointensity on the PVP and/or TP" and "hypointensity on the PVP and/or TP, and/or HBP" would lead to incorrect diagnoses of this lesion as an HCC

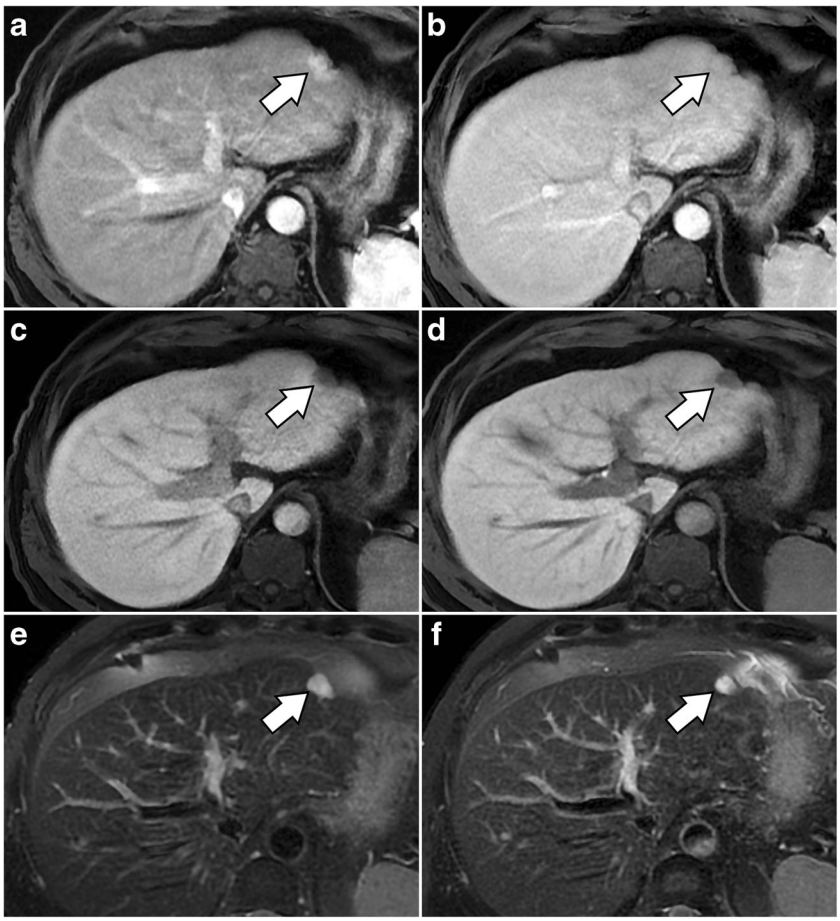

Fig. 4 A hemangioma in a 61-year-old male patient with chronic hepatitis B. (**a**) A small arterially enhancing nodule (*arrow*) is seen in the subcapsular area of the left lobe of the liver. This lesion shows isointensity relative to the liver parenchyma in the PVP images (**b**) and hypointensity in the TP (**c**) and HBP images (**d**). Imaging criterion of "arterial hyperenhancement and hypointensity on the PVP" would correctly diagnose this lesion as non-HCC; however, criteria of "hypointensity on the PVP and/or TP" and "hypointensity on the PVP and/or TP, and/or HBP" would lead to incorrect diagnoses of this lesion as an HCC. This lesion showed hyperintensity on the T2-weighted image (**e**), and 6-month follow-up MR image showed no interval change (**f**)

Table 3 Diagnostic Performances of Different Imaging Criteria for "Washout" on Gadoxetic Acid-Enhanced MRI for Hepatocellular Carcinoma: Subgroup Analysis of Histopathologically Confirmed Lesions

Imaging criteria	Sensitivity (%)	Specificity (%)	PPV (%)	NPV (%)	Accuracy (%)
Hyperenhancement on HAP					
+ Hypointensity on PVP	72.7 (93/128) [64.1-80.2]	91.7 (22/24) [73.0-98.7]	97.9 (93/95) [92.6-99.7]	38.6 (22/57) [26.0-52.4]	75.7 (115/152)
+ Hypointensity on PVP and/or TP	82.8 (106/128) [75.1-88.9]	58.3 (14/24) [36.7-77.9]	91.4 (106/116) [84.7-95.8]	38.9 (14/36) [23.2-56.5]	78.9 (120/152)
+ Hypointensity on PVP and/or TP, and/or HBP	91.4 (117/128) [85.1-95.6]	33.3 (8/24) [15.7-55.3]	88.0 (117/133) [81.2-93.0]	42.1 (8/19) [20.3-66.5]	82.2 (125/152)

Note: Numbers in parentheses were used to calculate percentages. Numbers in square brackets are 95 % confidence intervals. *HAP*=hepatic arterial phase, *PVP*=portal-venous phase, *TP*=transitional phase, *HBP*=hepatobiliary phase, *PPV*=positive predictive value, *NPV*=negative predictive value

revealed similar trends of sensitivity, specificity, and accuracy with the analysis of the whole study group.

Discussion

For the noninvasive diagnosis of HCC based on "hypervascularity in the HAP and washout on a later phase", our retrospective cohort study demonstrated that the criterion of "hypointensity on the PVP" of gadoxetic acid-enhanced MRI resulted in a high specificity of 97.9 %, while the criteria of "hypointensity on the PVP and/or TP" and "hypointensity on the PVP and/or TP, and/or HBP" resulted in lower specificities of 86.3 % and 48.4 %, respectively. Considering the clinical importance of obtaining a specific diagnosis of HCC, these results suggest that washout should be assessed in the PVP alone rather than combined with the TP or HBP for a more specific diagnosis of HCCs on gadoxetic acid-enhanced MRI [31]. Obtaining a specific diagnosis of HCC, i.e. minimizing false positives, is of critical importance in clinical practice because a false positive diagnosis of HCC can result in inappropriate or unnecessary treatment in patients with non-HCC malignant lesions or benign lesions, as well as unfair priority granting for liver transplantations [32]. Thus, a stringent diagnostic criterion is required for the noninvasive diagnosis of HCCs [32]. This is also why contrast enhanced ultrasound which has been reported to cause false positive HCC diagnoses in patients with cholangiocarcinoma has been eliminated from the 2010 AASLD guidelines [33]. As the current guidelines based on the typical vascular pattern has been reported to allow a correct diagnosis of HCCs with a predicted specificity of 95 % using ECCM-enhanced imaging [34, 35], our results of gadoxetic acid-enhanced MRI showing a specificity of 97.9 % based on the criterion of "hypointensity on the PVP" suggest that gadoxetic acid-enhanced MRI can also be used to evaluate the vascular pattern of hepatic nodules for the diagnosis of HCC. This specificity is also comparable to the specificities (96 – 97 %) of ECCM-enhanced CT or MRI [36, 37].

As for the sensitivity of gadoxetic acid-enhanced MRI in the diagnosis of HCCs, our study showed that relative hypointensity of the tumour was present in 70.9 % on the PVP and 86.0 % on the TP, which is comparable to a recent study on ECCM-enhanced MRI showing sensitivities of 44 % with PVP and 82 % with the delayed phase [38]. In addition, 93.8 % of HCCs in our study were seen as hypointense lesions on the HBP. Owing to the high percentage of HCCs showing hypointensity on the HBP, the criterion of "hypointensity on the PVP and/or TP, and/or HBP" resulted in high sensitivity. However, that criterion also resulted in low specificity as many non-HCC lesions which lacked normal hepatocytes would show hypointensity on the HBP. Therefore, we conclude that the HBP should not be used as a phase for assessing "washout" owing to its low specificity.

In our study, 13 non-HCCs showed hypointensity relative to the liver parenchyma on the TP. This resulted in a number of false positives when applying the criterion of "hypointensity on the PVP and/or TP." As hemangioma is the most common benign hepatic neoplasm and usually does not require treatment, accurate imaging diagnosis of hemangioma is of importance [18]. While hemangiomas typically show delayed retention of contrast media on ECCM-enhancing imaging [39], our study demonstrated that three hemangiomas were seen to be hypointense on the TP of gadoxetic acid-enhanced MRI. This result is in good agreement with previous studies by Doo et al. [19] which reported that high-flow hemangioma may show the "pseudo-washout" sign during the TP. Tateyama et al. [18] also reported that prolonged enhancement of hepatic hemangioma was less frequent on gadoxetic-acid enhanced MRI (52 %) than contrast-enhanced CT (100 %). This observed hypointensity of hemangioma on the TP can be due to the uptake of gadoxetic acid by the surrounding liver parenchyma, the lower dose of gadolinium, and the shorter plasma half-life of gadoxetic acid [40]. Interestingly, hypointensity on the PVP and/or TP of high-flow hemangioma has also been reported on gadobenate

dimeglumine (another hepatocyte-specific contrast agent)-enhanced MRI [41]. There were other false positives on the TP in addition to hemangioma including malignant lesions such as cHCC-CCs which will be described later, cholangiocarcinomas, and metastases. As for intrahepatic cholangiocarcinomas in the cirrhotic liver, it would be more frequently hypervascular than those in the normal liver [42], and thus is already known as a common mimicker of HCCs. Rimola et al. [43] suggested that the absence of washout of cholangiocarcinomas in the cirrhotic livers on the delayed phase of gadodiamide (an ECCM)-enhanced MRI may help avoid a potential misdiagnosis. However, as our results demonstrated, hypervascular intrahepatic cholangiocarcinomas can show hypointensity in the TP of gadoxetic acid-enhanced MRI. Peporte et al. [44] also reported that cholangiocarcinoma can be seen as a hypointense nodule on the TP.

Finally, we found that using the criterion of "hypointensity on the PVP", two non-HCCs were diagnosed as HCCs. These two false positive cases in our study were confirmed as cHCC-CCs. None of the benign lesions showed hypointensity on the PVP. As cHCC-CC is histologically composed of elements from both entities, its vascular pattern on contrast-enhanced imaging depends on the proportion of the tumour components [45, 46]. Therefore, an HCC-dominant tumour can show arterial hypervascularity and washout on a later phase mimicking an HCC, leading to a false positive diagnosis even with CT or ECCM-enhanced MRI [47, 48]. However, as patients with cHCC-CC have been reported to respond differently to therapy and that the prognoses after liver transplantation are poorer than those with HCC [49–51], differentiating cHCC from HCC would be very important in the establishing noninvasive diagnostic criteria. Therefore, further studies are warranted to differentiate cHCC-CCs from HCCs using imaging features.

This study has several limitations. First, as our study was performed retrospectively, there may have been selection bias in our patient population. However, we put our best effort to collect study patients in a consecutive cohort in order to avoid or minimize selection bias. Second, histological diagnoses were not available for a substantial number of benign non-HCCs. As performing biopsy for non-HCC lesions showing characteristic imaging features of common benign lesions may be unethical, characteristic imaging findings and follow-ups with CT or MRI were used for confirmation of the diagnosis. Third, as not all patients underwent ECCM-enhanced CT or MRI and gadoxetic acid-enhanced MRI within a short interval, we were not able to compare the diagnostic performances of the two imaging techniques and thus further study would be warranted in this regard. Fourth, we solely focused on the hemodynamic pattern of gadoxetic acid-enhanced MRI, and did not assess the role of ancillary features. Considering that static MRI sequences such as T2-weighted imaging and DWI with apparent diffusion coefficient (ADC) mapping can provide additional information other than just the hemodynamic pattern, the performance of MRI in diagnosing HCC using criteria including these ancillary features may be different from our study results.

In conclusion, when gadoxetic acid-enhanced MRI is used for the noninvasive diagnosis of HCC based on "hypervascularity on the HAP and washout on a later phase," washout should be determined on the PVP alone rather than combined with hypointensity on the TP or HBP in order to maintain high specificity.

Acknowledgments The scientific guarantor of this publication is Jeong Min Lee. The authors of this manuscript declare no relationships with any companies, whose products or services may be related to the subject matter of the article. No complex statistical methods were necessary for this paper.

This study was approved by the institutional review board of Seoul National University Hospital. Written informed consent was waived by the institutional review board. None of the study subjects or cohorts have been previously reported. Methodology: retrospective, diagnostic or prognostic study, performed at one institution. We thank Chris Woo, B.A. for his editing.

References

1. Tang A, Cruite I, Sirlin CB (2013) Toward a standardized system for hepatocellular carcinoma diagnosis using computed tomography and MRI. Expert Rev Gastroenterol Hepatol 7:269–279
2. Bruix J, Sherman M (2011) Management of hepatocellular carcinoma: an update. Hepatology 53:1020–1022
3. Bota S, Piscaglia F, Marinelli S, Pecorelli A, Terzi E, Bolondi L (2012) Comparison of International Guidelines for Noninvasive Diagnosis of Hepatocellular Carcinoma. Liver Cancer 1:190–200
4. European Association For The Study Of The Liver, European Organisation For Research And Treatment Of Cancer (2012) EASL-EORTC clinical practice guidelines: management of hepatocellular carcinoma. J Hepatol 56:908–943
5. Forner A, Llovet JM, Bruix J (2012) Hepatocellular carcinoma. Lancet 379:1245–1255
6. Kim SH, Lee J, Kim MJ et al (2009) Gadoxetic acid-enhanced MRI versus triple-phase MDCT for the preoperative detection of hepatocellular carcinoma. AJR Am J Roentgenol 192:1675–1681
7. Inoue T, Kudo M, Komuta M et al (2012) Assessment of Gd-EOB-DTPA-enhanced MRI for HCC and dysplastic nodules and comparison of detection sensitivity versus MDCT. J Gastroenterol 47:1036–1047
8. Park G, Kim YK, Kim CS, Yu HC, Hwang SB (2010) Diagnostic efficacy of gadoxetic acid-enhanced MRI in the detection of hepatocellular carcinomas: comparison with gadopentetate dimeglumine. Br J Radiol 83:1010–1016
9. Sano K, Ichikawa T, Motosugi U et al (2011) Imaging study of early hepatocellular carcinoma: usefulness of gadoxetic acid-enhanced MR imaging. Radiology 261:834–844
10. Kudo M (2010) Will Gd-EOB-MRI change the diagnostic algorithm in hepatocellular carcinoma? Oncology 78(Suppl 1):87–93
11. Kudo M, Izumi N, Kokudo N et al (2011) Management of hepatocellular carcinoma in Japan: Consensus-Based Clinical Practice Guidelines proposed by the Japan Society of Hepatology (JSH) 2010 updated version. Dig Dis 29:339–364
12. Bashir MR, Gupta RT, Davenport MS et al (2013) Hepatocellular carcinoma in a North American population: does hepatobiliary MR

imaging with Gd-EOB-DTPA improve sensitivity and confidence for diagnosis? J Magn Reson Imaging 37:398–406
13. Palmucci S (2014) Focal liver lesions detection and characterization: The advantages of gadoxetic acid-enhanced liver MRI. World J Hepatol 6:477–485
14. Lee JM, Zech CJ, Bolondi L et al (2011) Consensus report of the 4th International Forum for Gadolinium-Ethoxybenzyl-Diethylenetriamine Pentaacetic Acid Magnetic Resonance Imaging. Korean J Radiol 12: 403–415
15. Sun HY, Lee JM, Shin CI et al (2010) Gadoxetic acid-enhanced magnetic resonance imaging for differentiating small hepatocellular carcinomas (< or =2 cm in diameter) from arterial enhancing pseudolesions: special emphasis on hepatobiliary phase imaging. Investig Radiol 45:96–103
16. Motosugi U, Ichikawa T, Sou H et al (2010) Distinguishing hypervascular pseudolesions of the liver from hypervascular hepatocellular carcinomas with gadoxetic acid-enhanced MR imaging. Radiology 256:151–158
17. Kudo M (2011) Diagnostic imaging of hepatocellular carcinoma: recent progress. Oncology 81(Suppl 1):73–85
18. Tateyama A, Fukukura Y, Takumi K et al (2012) Gd-EOB-DTPA-enhanced magnetic resonance imaging features of hepatic hemangioma compared with enhanced computed tomography. World J Gastroenterol 18:6269–6276
19. Doo KW, Lee CH, Choi JW, Lee J, Kim KA, Park CM (2009) "Pseudo washout" sign in high-flow hepatic hemangioma on gadoxetic acid contrast-enhanced MRI mimicking hypervascular tumor. AJR Am J Roentgenol 193:W490–W496
20. Kim SS, Hwang JC, Lim SG, Ahn SJ, Cheong JY, Cho SW (2014) Effect of virological response to entecavir on the development of hepatocellular carcinoma in hepatitis B viral cirrhotic patients: comparison between compensated and decompensated cirrhosis. Am J Gastroenterol 109:1223–1233
21. An C, Park MS, Kim D et al (2013) Added value of subtraction imaging in detecting arterial enhancement in small (<3 cm) hepatic nodules on dynamic contrast-enhanced MRI in patients at high risk of hepatocellular carcinoma. Eur Radiol 23:924–930
22. Nino-Murcia M, Olcott EW, Jeffrey RB Jr, Lamm RL, Beaulieu CF, Jain KA (2000) Focal liver lesions: pattern-based classification scheme for enhancement at arterial phase CT. Radiology 215:746–751
23. Jelic S, Sotiropoulos GC (2010) Hepatocellular carcinoma: ESMO Clinical Practice Guidelines for diagnosis, treatment and follow-up. Ann Oncol 21(Suppl 5):v59–v64
24. Oto A, Kulkarni K, Nishikawa R, Baron RL (2010) Contrast enhancement of hepatic hemangiomas on multiphase MDCT: Can we diagnose hepatic hemangiomas by comparing enhancement with blood pool? AJR Am J Roentgenol 195:381–386
25. Vilanova JC, Barcelo J, Smirniotopoulos JG et al (2004) Hemangioma from head to toe: MR imaging with pathologic correlation. Radiographics 24:367–385
26. Ahn JH, Yu JS, Hwang SH, Chung JJ, Kim JH, Kim KW (2010) Nontumorous arterioportal shunts in the liver: CT and MRI findings considering mechanisms and fate. Eur Radiol 20:385–394
27. Gabata T, Kadoya M, Matsui O et al (2001) Dynamic CT of hepatic abscesses: significance of transient segmental enhancement. AJR Am J Roentgenol 176:675–679
28. Byun JH, Yang DH, Yoon SE et al (2006) Contrast-enhancing hepatic eosinophilic abscess during the hepatic arterial phase: a mimic of hepatocellular carcinoma. AJR Am J Roentgenol 186:168–173
29. Grieser C, Steffen IG, Seehofer D et al (2013) Histopathologically confirmed focal nodular hyperplasia of the liver: gadoxetic acid-enhanced MRI characteristics. Magn Reson Imaging 31:755–760
30. Yoon SH, Lee JM, So YH et al (2009) Multiphasic MDCT enhancement pattern of hepatocellular carcinoma smaller than 3 cm in diameter: tumor size and cellular differentiation. AJR Am J Roentgenol 193:W482–W489
31. Forner A, Vilana R, Ayuso C et al (2008) Diagnosis of hepatic nodules 20 mm or smaller in cirrhosis: Prospective validation of the noninvasive diagnostic criteria for hepatocellular carcinoma. Hepatology 47:97–104
32. Hayashi PH, Trotter JF, Forman L et al (2004) Impact of pretransplant diagnosis of hepatocellular carcinoma on cadveric liver allocation in the era of MELD. Liver Transpl 10:42–48
33. Barreiros AP, Piscaglia F, Dietrich CF (2012) Contrast enhanced ultrasound for the diagnosis of hepatocellular carcinoma (HCC): comments on AASLD guidelines. J Hepatol 57:930–932
34. Sangiovanni A, Manini MA, Iavarone M et al (2010) The diagnostic and economic impact of contrast imaging techniques in the diagnosis of small hepatocellular carcinoma in cirrhosis. Gut 59:638–644
35. El-Serag HB, Marrero JA, Rudolph L, Reddy KR (2008) Diagnosis and treatment of hepatocellular carcinoma. Gastroenterology 134: 1752–1763
36. Liu YI, Kamaya A, Jeffrey RB, Shin LK (2012) Multidetector computed tomography triphasic evaluation of the liver before transplantation: importance of equilibrium phase washout and morphology for characterizing hypervascular lesions. J Comput Assist Tomogr 36: 213–219
37. Marrero JA, Hussain HK, Nghiem HV, Umar R, Fontana RJ, Lok AS (2005) Improving the prediction of hepatocellular carcinoma in cirrhotic patients with an arterially-enhancing liver mass. Liver Transpl 11:281–289
38. Cereser L, Furlan A, Bagatto D et al (2010) Comparison of portal venous and delayed phases of gadolinium-enhanced magnetic resonance imaging study of cirrhotic liver for the detection of contrast washout of hypervascular hepatocellular carcinoma. J Comput Assist Tomogr 34:706–711
39. Burkholz KJ, Silva AC (2008) AJR teaching file: hypervascular metastasis or hepatic hemangioma? AJR Am J Roentgenol 190:S53–S56
40. Ringe KI, Husarik DB, Sirlin CB, Merkle EM (2010) Gadoxetate disodium-enhanced MRI of the liver: part 1, protocol optimization and lesion appearance in the noncirrhotic liver. AJR Am J Roentgenol 195:13–28
41. Quaia E, Pizzolato R, De Paoli L, Angileri R, Ukmar M, Cova MA (2013) Arterial enhancing-only nodules less than 2 cm in diameter in patients with liver cirrhosis: predictors of hepatocellular carcinoma diagnosis on gadobenate dimeglumine-enhanced MR imaging. J Magn Reson Imaging 37:892–902
42. Xu J, Igarashi S, Sasaki M et al (2012) Intrahepatic cholangiocarcinomas in cirrhosis are hypervascular in comparison with those in normal livers. Liver Int 32:1156–1164
43. Rimola J, Forner A, Reig M et al (2009) Cholangiocarcinoma in cirrhosis: absence of contrast washout in delayed phases by magnetic resonance imaging avoids misdiagnosis of hepatocellular carcinoma. Hepatology 50:791–798
44. Peporte AR, Sommer WH, Nikolaou K, Reiser MF, Zech CJ (2013) Imaging features of intrahepatic cholangiocarcinoma in Gd-EOB-DTPA-enhanced MRI. Eur J Radiol 82:e101–e106
45. Chung YE, Park MS, Park YN et al (2009) Hepatocellular carcinoma variants: radiologic-pathologic correlation. AJR Am J Roentgenol 193:W7–W13
46. Fukukura Y, Taguchi J, Nakashima O, Wada Y, Kojiro M (1997) Combined hepatocellular and cholangiocarcinoma: correlation between CT findings and clinicopathological features. J Comput Assist Tomogr 21:52–58
47. Fowler KJ, Sheybani A, Parker RA 3rd et al (2013) Combined hepatocellular and cholangiocarcinoma (biphenotypic) tumors: imaging features and diagnostic accuracy of contrast-enhanced CT and MRI. AJR Am J Roentgenol 201:332–339

48. Sanada Y, Shiozaki S, Aoki H, Takakura N, Yoshida K, Yamaguchi Y (2005) A clinical study of 11 cases of combined hepatocellular-cholangiocarcinoma Assessment of enhancement patterns on dynamics computed tomography before resection. Hepatol Res 32:185–195
49. Teefey SA, Hildeboldt CC, Dehdashti F et al (2003) Detection of primary hepatic malignancy in liver transplant candidates: prospective comparison of CT, MR imaging, US, and PET. Radiology 226:533–542
50. Lee WS, Lee KW, Heo JS et al (2006) Comparison of combined hepatocellular and cholangiocarcinoma with hepatocellular carcinoma and intrahepatic cholangiocarcinoma. Surg Today 36:892–897
51. Patel T (2011) Cholangiocarcinoma–controversies and challenges. Nat Rev Gastroenterol Hepatol 8:189–200